Predictive Analytics for Non-stationary V2I Channel

Mohanad Al-Ibadi
Department of Electrical Engineering and Computer Science
University of Kansas
Lawrence, KS 66045

Aveek Dutta
Department of Computer Engineering
University at Albany, SUNY
Albany, NY 12222

***Abstract*—Vehicle to Infrastructure (V2I) channels are particularly difficult to analyze because of high mobility and localized scattering from nearby vehicles and road-side features. The spatio-temporal variation of the scattering environment makes the channel a non-stationary stochastic process, which renders conventional, receiver-side channel conditioning techniques ineffective for this emerging application. Our work takes a radically different approach to introduce predictive analytics at the Road-Side Unit (RSU) to proactively compensate for channel variations over time and frequency while precisely fitting into contemporary protocols like Dedicated Short Range Communication (DSRC) and Wireless Access in Vehicular Environment (WAVE). By assimilating the channel state feedback built into these protocols, we employ an iterative learning algorithm to gather localized knowledge of the channel profile. This acquired knowledge is used to pre-condition the downlink waveform to lower the Bit Error Rate (BER) by ≈ 100 times, when compared to the current vehicular communication standards even at a relatively high Signal to Noise (SNR) of 17 dB. Further, our algorithm is able to predict the non-stationary V2I channel with an average absolute error of 10^{-2} in dense scattering environment.**

I. Introduction

Edge networks and connected car: The recent explosion of interest in autonomous vehicles [1] necessitate an overhaul of vehicular networks. While the main focus remains on disseminating safety and traffic related information [2], the infrastructure has to be robust for broadband communication as well. This is further motivated by the fact that existing wireless infrastructures are increasingly constrained on resources to make new allocations towards the network edge [3], [4]. Figure 1 shows the topology of a vehicular Edge network [3], [4], which consists of radio transceivers installed in the vehicles and the Road-Side Unit (RSU), which is equivalent to an access point (AP) or eNodeB (eNB). Apart from providing connectivity to the vehicles, the RSU is equipped with storage and compute resources as well [5], [6]. This enables network architects to build intelligent vehicular networks that are fast, proactive and efficient.

Intelligence is required at every level of Edge networks, whether it is mitigating the impairments in the wireless channel or proactive caching of content based on when and where it is needed. Vehicular networks are unique because the communicating nodes (either vehicle-to-vehicle (V2V) or vehicle-to-infrastructure (V2I) [7]) are always moving relative to the other. Consequently, the wireless channel is extremely volatile, which is a combination of many factors like, Doppler shift, shadowing, scattering (large and small scale), etc. More importantly, all of these quantities are time-varying and statistically non-stationary [8], [9]. This non-stationarity of the channel lends a unique dimension to this application that is unseen in conventional broadband wireless networks.

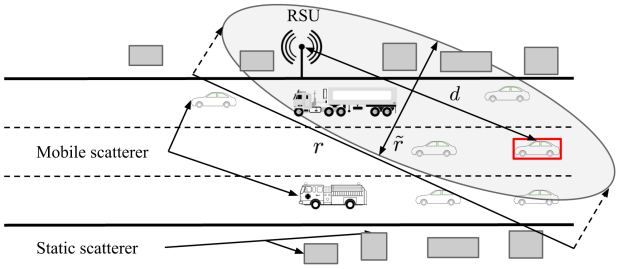

Figure 1: Example of a vehicular Edge network: The scattering environment (shown by the ellipse and detailed in §II) between the RSU and the vehicle is comprised of stationary and mobile scatterers, making the channel non-stationary over time and frequency.

In this work, we create a localized model of the V2I wireless channel using iterative learning methods (detailed in §III and §IV) making the V2I channel more reliable. This, in turn, enables a broader set of reliable network services, like traffic-aware caching, multi-user downlink scheduling and coordinated dissemination of vehicular safety messages.

Predictive analytics at RSU: Figure 2a shows an example of a V2I channel across time and frequency. The frequency selectivity of the V2I channel, as shown in Figure 2a, pose great challenge for broadband communication using frequency domain modulation such as Orthogonal Frequency Division Multiplexing (OFDM). Furthermore, the standards advocated for WAVE [10] are based on Dedicated Short Range Communication (DSRC) messages that are not robust enough to compensate for the rich fading environment [11]. These waveforms preserve much of the PHY and MAC layer parameters from common wireless standards like 802.11a/g [12].

Now, assuming a vehicle is moving at 50 miles/hr (or 22 meters/sec), the maximum Doppler shift is, $(f_D)_{max} = v/\lambda_c = 438$ Hz, for a center frequency of 5.9 GHz. Therefore, the channel coherence time, which provides a measure of how fast the channel is changing over time, is, $T_{coh} = 1/(2\pi f_d) \approx 363\mu s$; With the PHY parameters of 802.11p (WAVE), the coherence time T_{coh} translates to 43 OFDM symbols ($8\mu s$/symbol). If we assume that the channel condition can support QPSK-3/4 modulation and coding (or

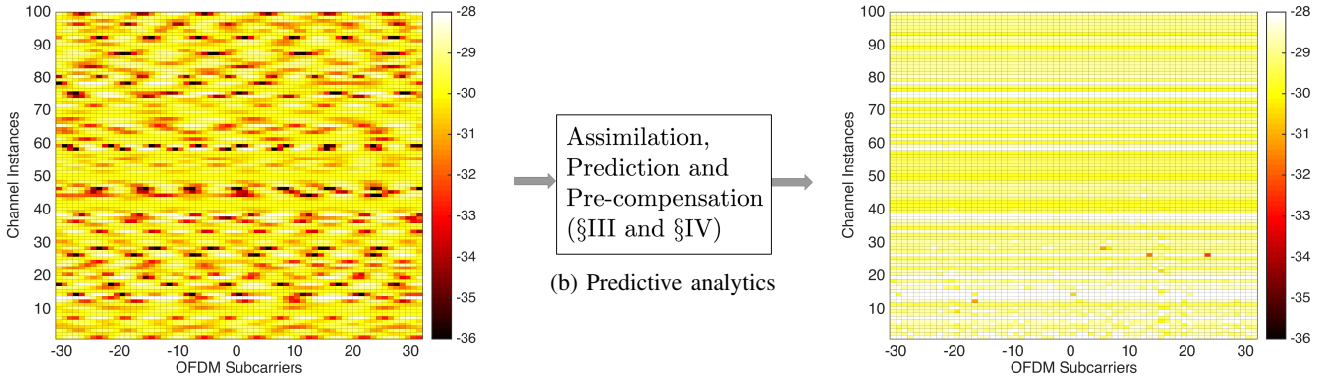

(a) Channel profile over time and frequency

(b) Predictive analytics

(c) Channel profile with predictive analytics

Figure 2: High level system performance: a) Non-stationary, frequency selective, vehicle density dependent channel is reported as CSI feedback by the vehicles, which serves as the input to the predictive analytics system. b) The analytics engine employs a combination of iterative learning and pre-compensation algorithms to accurately predict the channel for future communications. This is the main contribution of this work. c) The accurate prediction and pre-compensation at the RSU leads to uniform and flat fading across time and frequency when estimated at the vehicle, making V2I communications highly reliable.

18 Mbps), which allows for 72 uncoded data bits per OFDM symbol, a 1KB payload will require 85 OFDM symbols.

Observation 1: *The coherence time of a typical V2I channel is **less** than the duration of a 1KB packet.*

Furthermore, the coherence bandwidth B_{coh}, which is a measure of channel impairment in the frequency domain, is expressed as $B_{coh} = 1/(2\pi\tau_{rms}) = 800KHz$, assuming, $\tau_{rms} = 2T_s = 200ns$ [13], where T_s is the sample time . Now, 800 KHz spans $B_{coh}/\Delta f \approx 5$ subcarriers (Δf = subcarrier spacing in 802.11p is 156.25KHz), which means that in frequency domain the channel changes every 5 subcarriers, while the pilot spacing in 802.11p is 14. In other words, the channel changes faster than the frequency of occurrence of the pilot carriers used for estimating the channel.

Observation 2: *The widely implemented pilot based channel estimation is **unable** to track the wireless channel in frequency domain as it changes, often drastically, as shown in Figure 2a over time and frequency.*

Role of Channel State Information (CSI): CSI in OFDM based systems, can be interpreted as the time-average of the estimated frequency domain channel coefficients at the receiver over the duration of a packet (many OFDM symbols). Therefore, a CSI information comprises of real and imaginary values for all the subcarriers (typically represented by 12 to 16 bits in a fixed point implementation of a transceiver). In vehicular networks like 802.11p, this CSI information can be easily piggy-backed onto the acknowledgment frames without any modification to the protocol. Therefore, the CSI is essentially a feedback information from the vehicles that capture the fading profile of the downlink (RSU to vehicles) channel. Although not currently implemented, we believe that it is straightforward to add 256 bytes (64 subcarriers $\times$ 16 bits/subcarrier $\times$ 2 (I/Q components)) to an acknowledgment frame while preserving compatibility with legacy protocols.

This information is used by the RSU to tune the transmission parameters (rate adaptation) of future packets. However, this is feasible only if the channel is changing at a slow rate. From Observations 1 and 2 above, it is evident that V2I channels are an exception to this. Simply because the channel characteristics change drastically over the duration of a single packet and the pilot subcarriers are unable to track the channel in frequency domain, which leads to increased packet error rate (PER) at the higher layers. By the time the CSI arrives at the RSU, piggy-backed on the acknowledgment frame, the channel has already changed to a new state and the previous observation is rendered ineffective for any adaptive transmission. Therefore, we incorporate intelligence at the RSU to learn the unique fading environment for a particular segment of the road (in order of tens of meters) over time based on the CSI received from vehicles. With knowledge of the fading profile of that segment of road, future downlink OFDM transmission is pre-compensated at the RSU, thus nulling the effects of the channel impairment as it travels to the vehicles. Since every acknowledgment frame will potentially have a CSI payload, over time the system captures a wide range of channel dynamics that is assimilated to build localized knowledge about the fading profile of the V2I channel. Predictive analytics, using large number of CSI measurements facilitates linear channel estimation and equalization at the vehicles to produce a flat response across the subcarriers, as shown in Figure 2c, which ultimately improves the BER (discussed in §V). The main contributions of this paper are:

1) Emulate a realistic vehicular Edge network by combining Geometry-based Stochastic Channel Model (GSCM) and appropriate scattering environment (§II). This allows us to model the vehicular fading environment based on spatio-temporal variation of small and large scale scatterers.

2) Assimilate the CSI information from the vehicles and design a Kalman filter based prediction mechanism along with autoregression smoothing to track the non-stationary V2I channel (§III).
3) Pre-compensate the downlink OFDM waveform at the RSU using the predicted channel to compensate for the frequency selective fading. This results in superior estimation and equalization at the vehicles, improving the BER (§IV).
4) Using these predictive analytics at the RSU, the non-stationary V2I channel is tracked with high accuracy and the BER is lowered by almost two orders of magnitude compared to conventional receiver side algorithms (§V).

II. System Model

Consider the vehicular environment shown in Figure 1, where a single-antenna RSU of height d_{RSU} above the ground is placed at the center of a road of length d_{road}. The RSU is communicating with a single vehicle equipped with a single isotropic antenna through a multipath environment, and we assume a line-of-sight (LOS) link is always present. The target vehicle (vehicle in red box in Figure 1) is assumed to be moving with a constant speed V along the road, while other vehicles are moving with varying speeds and they act as scatterers. The road is divided into several *segments*, where each segment represents a *scenario* that has its own unique propagation characteristics. A channel segment is a period of quasi-stationarity, during which the probability distributions of the large scale scatterers, like road-side features, do not change noticeably [14]. In each segment, there are two types of scatterers: *fixed scatterers*, which are usually along the side of the road, such as the buildings and sign posts, and *variable scatterers*, which are usually on the road, such as vehicles and motorcycles (we neglect the effect of pedestrians). For the i^{th} segment, let n_{f_i}, n_{v_i}, and $n_{\max_i}$ represent the number of fixed objects, number of variable objects, and the maximum number of possible variable objects respectively (assuming that all segments have the same length d_{seg}), then the total number of scatterers (or objects) in segment i is: $N_{scat}^{(i)} = n_{f_i} + n_{v_i}, \quad 1 \leq i \leq N_{seg}$ where, N_{seg} is the number of segments of the road, and $0 \leq n_{v_i} \leq n_{\max_i}$. Note that, n_{f_i} is a fixed scalar, while n_{v_i} is a random variable whose expected value is a measure of the vehicle density in segment i. Each time N_{scat} changes, some of the large scale parameters (LSPs) and small scale parameters (SSPs) also change accordingly that results in a new and unique channel profile (coefficients) and thus, new power-delay and power-frequency profiles as well. Keeping track of these unique channel realizations and extracting the underlying model parameters is the goal of this work.

Scattering Zone: Each scattering zone represents a single-link connecting the transmitter and the receiver and is geometrically represented as an ellipse [14] . If the transmitter (TX) and receiver (RX) are at the foci of an ellipse with distance d between them (TX-RX distance), and r is the maximum communication range based on their transmit power (i.e. r is the major radius of the ellipse), then $\tilde{r} = \sqrt{r^2 - d^2}/2$ is the minor ellipse's diameter [9]. Based on the values of r and d, we define the following extremes of the scattering environment:

1) Zero Scattering Region (ZSR): If $r \approx d$, then $\tilde{r} \approx 0$ the RSU (as in Figure 1) is communicating with a vehicle at the beginning of the road (i.e. leftmost and rightmost segments). At these locations, the ellipse is approximately a line (area ≈ 0) and we can assume that the RSU and the vehicle are only connected via a LOS link. Intuitively, this means that there is no scattering in this region as the line LOS components dominates the fading profile.

2) Full Scattering Region (FSR): If $r >> d$, then $\tilde{r} \approx r/2$, and the ellipse is approximately a circle. This case happens when the vehicle is close to the RSU and maximum scattering is experienced from neighboring vehicles.

In this work, we consider the FSR scenario to design predictive algorithms and measure the BER performance.

A. Non-stationarity of the V2I Channel

V2I channels are modeled as GSCM, which forms the basis of the widely used WINNER channel model [14]. The channel at time k and for the n^{th} OFDM subcarrier is given by

$$h(k,n) = \sum_{\ell=1}^{N_{scat}(k)} h(k,n,\ell) \text{ where,} \tag{1}$$

$$h(k,n,\ell) = \sum_{m=1}^{M_\ell} \alpha_m(k,n) e^{j\varphi_m(k,n)} e^{j2\pi f_{D_m}(k,n)k} \delta(\tau - \tau_m(k,n))\delta(\theta - \theta_m(k,n))\delta(\phi - \phi_m(k,n)) \tag{2}$$

where, $N_{scat}(k)$ is the number of scatterers as a function of time assuming that at each time k, each resolvable path corresponds to one scatterer, and M is the number of sub-paths constituting each ray. $\alpha_m(k,n)$ is the complex channel gain at time k and subcarrier n. $\phi_m(k,n)$ and $\theta_m(k,n)$ are the angle of departure (AoD) and the angle of arrival (AoA) of the m^{th} sub-path respectively, as a function of time and frequency. The AoAs and AoDs are functions of the RSU location (fixed), vehicle location, and the distribution of the scatterers in each scattering zone. $f_{D_m}(k,n)$ is the Doppler frequency which is assumed to be constant in our work (constant speed of vehicle reporting CSI). $\tau_m(k,n)$ is the path delay measured at time k for subcarrier n and depends on the scatterers locations, which are stochastically distributed in the scattering zone. Therefore, *the channel dynamics are functions of the number of scatterers and their locations with respect to the RSU and the vehicle, and the vehicle speed.*

Figure 3 shows an example of the non-stationarity of the V2I channel. Figure 3a shows the time varying statistics (median and variance) for different number of vehicles around the vehicle reporting the CSI. Figure 3b shows the variance of the channel magnitude (averaged over all subcarriers) for a constant vehicle density, which is also a function of time. Finally, Figure 3c shows the frequency domain representation of the V2I channel over time for a segment in the center of the road with FSR and 13 scatterers (vehicles and road-side

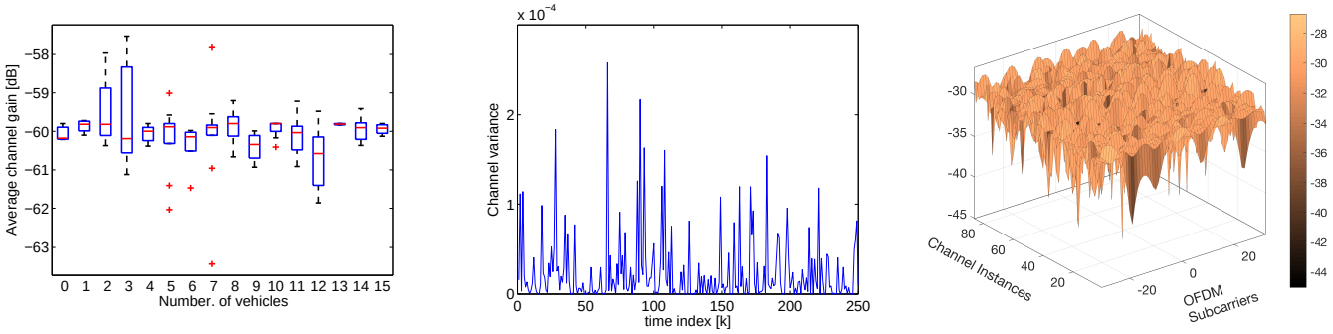

(a) Distribution of channel gain (b) Variance of channel gain over time (c) Example channel profile $N_{scat}^{(i)} = 13$

Figure 3: Non-stationarity of the V2I channel over time, frequency and vehicle density for a given segment of the road: a) Non-stationarity with number of scatterers: The median and variance of the channel gain (averaged over all subcarriers) changes with the number of scatterers. b) Non-stationarity over time: The channel variance is a function of time for the same number of scatterers and c) Example realization of the non-stationary channel

feature combined). The goal is to predict this channel profile at the RSU and then pre-condition the waveform to offset the effect of such impairment. The following sections discuss the steps to alleviate the effects of such non-stationarity.

III. Assimilation and Prediction

The need for channel prediction arises from the fact that by the time the vehicle estimates the channel state and sends it back to the RSU, the vehicle has already moved to another location, and the CSI will no longer be useful for adapting downlink transmission (i.e. outdated channel). This is because the channel is different at each location that depends on the LSPs, SSPs, and the area of the scattering zone along with path-loss and Doppler shift. The V2I channel, as represented by (1) is a linear system, which makes Kalman filter particularly well-suited for tracking and predicting the channel statistics. However, in our design, we do not track the channel coefficients (per subcarrier) using the Kalman filter. Instead the predicted channel coefficients are combined by an autoregressive (AR) model and the weights of the AR model are tracked and predicted by the Kalman filter. For each location, the RSU stores the channel states whenever it is available, as shown in Table I. Note that the number of scatterers is continuously changing (as the vehicles enter/exit the road). Thus, we expect that the channel states to be different over time for the same location. Even if it happens that the environment is the same, the noise variance will be different due to non-stationarity. Thus, the degree of correlation between two data samples at a given location is a function of the environment, and potentially is very small. We assume that in an Intelligent Transportation Systems (ITS) the RSU will have complete knowledge of the topology (location, speed, heading, etc) as well as the LSPs based on widely available Geographical Information Systems (GIS). In our analysis, we assume that the there is only one lane in each direction and the path-loss is the same along the major axis of the elliptical scattering zone as shown in Figure 1. The prediction system operates in real-time and does not require any training data making it suitable for high data rate broadband downlink communication.

Table I: Database for each *segment* i stored at the RSU

Time	Speed	Scattering Info.	CSI	Assimilate CSIs over time ⇓ Output: predicted downlink channel for segment i
time 1	V_1	LSP 1, N_{scat}^1	CSI 1	
time 2	V_2	LSP 2, N_{scat}^2	CSI 2	
⋮	⋮	⋮	⋮	
time N	V_K	LSP N, N_{scat}^K	CSI K	

A. Tracking the V2I Channel

Autoregression (AR) is used to model the unknown structure of a time series consisting of a set of correlated data samples. However, AR model is only valid if the time series is a stationary random process. In the context of this problem, the channel is non-stationary over time, frequency, and vehicles density, as shown in Figure 3. Thus, a noisy AR-model (i.e random walk process), is used to model the statistics of the non-stationary channel with a model order p . In general, for a given stationary time series, the future data instances can be modeled as a weighted sum of the p previous data samples

$$z(k) = \sum_{i=1}^{p} a_i z(k-i) + u(k) \tag{3}$$

where, $\{a_i, 1 \leq i \leq p\}$ are the weights that represent the statistics of the time series, and $u(k)$ is an additive white noise.

Now, consider a random walk process represented as a discrete-time linear system with the following state-space representation (SSR) [15]

$$\mathbf{a}(k+1) = \mathbf{a}(k) + \mathbf{u}_1(k) \tag{4}$$

$$\mathbf{z}(k) = \mathbf{C}(k-1)\mathbf{a}(k) + \mathbf{u}_2(k) \tag{5}$$

Table II shows the meaning and dimensions of the variables used in this section. Equation (4) represents the system dynamics (or process) equation, where $\mathbf{a}(k)$ represents the statistics

of the channel realizations to be tracked using Kalman filter at time k for N subcarriers. On the other hand, equation (5) represents the observation (or measurement) equation. $\mathbf{C}(k-1)$ maps the state space into the observation space:

$$\mathbf{C}(k-1) = \text{diag}\{\mathbf{z}(k-1,n), 1 \leq n \leq N\} \tag{6}$$

where, $\mathbf{z}(k-1,n) = [z(k-1,n) \;\; z(k-2,n) \;\; \ldots \;\; z(k-p,n)]$ is a $1 \times p$ row vector contains the previous p CSI that were piggybacked on prior acknowledgment frames as recorded using Table I. Conventional methods of tracking the channel coefficients using Kalman filter assuming the channel statistics as time-invariant [16], [17]) is not suitable for vehicular networks due to the non-stationarity of the channel, as we showed in Figure 3. Instead, our method tracks the time-varying AR-parameters based on (4) and (5), and then use them to predict the future channel states using (7) – (14).

The formulation of the Kalman filter algorithm that is used to track and predict the AR-parameter, **a**(k) is as follows:

- Prediction step:

$$\mathbf{R}_{u_1}(k) = \mathbb{E}[\mathbf{u}_1(k)\mathbf{u}_1^H(k)] \tag{7}$$
$$\mathbf{R}_{u_2}(k) = \mathbb{E}[\mathbf{u}_2(k)\mathbf{u}_2^H(k)] \tag{8}$$
$$\mathbf{G}(k) = \mathbf{R}_c(k)\mathbf{C}^H(k-1) [\mathbf{C}(k-1)\mathbf{R}_c(k)\mathbf{C}^H(k-1) + \mathbf{R}_{u_2}(k)]^+ \tag{9}$$
$$\mathbf{R}_p(k) = \big(\mathbf{I} - \mathbf{G}(k)\mathbf{C}(k-1)\big)\mathbf{R}_c(k) \tag{10}$$

- Update (or correction) step:

$$\mathbf{a}(k+1) = \mathbf{a}(k) + \mathbf{G}(k)\big(\mathbf{z}(k) - \mathbf{C}(k-1)\mathbf{a}(k)\big) \tag{11}$$
$$\tilde{\mathbf{R}}_c(k+1) = \mathbf{R}_p(k) + \mathbf{R}_{u_1}(k) \tag{12}$$
$$\mathbf{R}_c(k+1) = \text{Triu}(\tilde{\mathbf{R}}_c(k+1)) \tag{13}$$

where, X^+ is the pseudo-inverse of matrix X, and $\text{Triu}(X)$ is the upper-triangular portion of matrix X. The upper-triangular portion of the state-error covariance matrix $\tilde{\mathbf{R}}_c(k)$ is used to compensate for numerical instability that is commonly encountered in Kalman filtering [18].

From (11), the predicted channel state is computed as:

$$\mathbf{z}_p(k) = \mathbf{C}(k-1)\mathbf{a}(k) \tag{14}$$

which is formed by a weighted sum of the previous p measurement channel-state vectors as in (3). Figure 4 shows the complete system including the Kalman filter. The *channel coefficient generator* and *channel pre-compensator* modules are discussed in the following section.

IV. Channel Pre-compensation at RSU

The goal of predicting the channel at the RSU is to pre-equalize the downlink packet such that the receiver estimates an almost flat fading over time and frequency, resulting in lower BER. This also eliminates the need for complex receiver-side equalization techniques and makes it easier to track the channel using the existing pilot carriers. Here, we focus on pre-compensating the the magnitude term of the

Table II: The variables used in Kalman filter algorithm

Variable	Dimension	Meaning
$\mathbf{a}(k)$	$pN \times 1$	AR-model coefficients vector
$\mathbf{u}_1(k)$	$pN \times 1$	Gaussian process noise vector $\mathbf{N}(0, \sigma_{u1}^2)$
$\mathbf{u}_2(k)$	$N \times 1$	Gaussian measurement noise vector $\mathbf{N}(0, \sigma_{u2}^2)$
$\mathbf{z}(k)$	$N \times 1$	Measurement channel vector
$\mathbf{z}_p(k)$	$N \times 1$	Predicted channel vector
$\mathbf{C}(k-1)$	$N \times pN$	Measurement matrix
$\mathbf{R}_{u_1}(k)$	$pN \times pN$	Process noise covariance matrix
$\mathbf{R}_{u_2}(k)$	$N \times N$	Measurement noise covariance matrix
$\mathbf{R}_p(k)$	$pN \times pN$	Predicted state-error covariance matrix
$\tilde{\mathbf{R}}_c(k+1)$	$pN \times pN$	Corrected state-error covariance matrix (Riccati update equation)
$\mathbf{R}_c(k+1)$	$pN \times pN$	Upper-triangular portion of $\tilde{\mathbf{R}}_c(k+1)$
$\mathbf{G}(k)$	$pN \times N$	Kalman gain matrix
$\mathbf{I}$	$pN \times pN$	Identity matrix

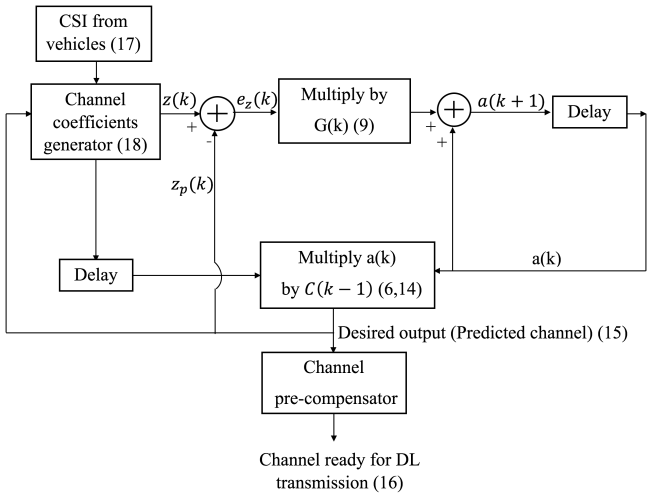

Figure 4: System model including Kalman filter (The corresponding equations are also indicated in parenthesis).

predicted channel in (14) only. Let the predicted channel for N subcarriers be,

$$\mathbf{z}_p(k) = \begin{bmatrix} z_p(k,1) & z_p(k,2) \ldots & z_p(k,N) \end{bmatrix}^T \tag{15}$$

Then, the pre-compensated predicted channel is,

$$\tilde{\mathbf{z}}_p(k) = \begin{bmatrix} \frac{1}{z_p(k,1)} & \frac{1}{z_p(k,2)} \cdots & \frac{1}{z_p(k,N)} \end{bmatrix}^T \tag{16}$$

Therefore, the resultant channel profile, $\mathbf{z}_f(k)$, as estimated by the vehicle while receiving a downlink packet is given by Hadamard product ($\odot$), which is equivalent to convolution in time-domain,

$$\mathbf{z}_f(k) = \mathbf{z}_t(k) \odot \tilde{\mathbf{z}}_p(k) + \mathbf{w}(k) \tag{17}$$

where $\mathbf{z}_t(k)$ refers to the true channel. $\mathbf{w}(k)$ is an additive term that captures the effect of the noise and estimation errors.

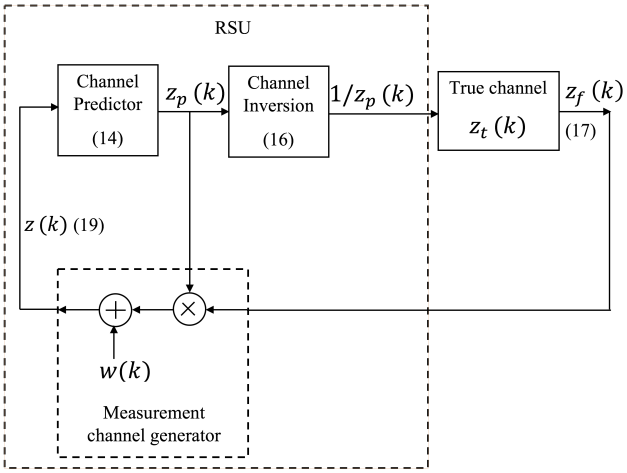

Figure 5: Measurement channel life-cycle: it shows how the true, measurement, predicted, and compensated channels are related to each other (The corresponding equations are also indicated in parenthesis).

Please note that $\mathbf{z}_t(k)$ is the fading profile of the V2I at instant k at a particular segment i and is an unknown quantity. In other words, the CSI, calculated at the vehicle captures the interaction between the true channel $\mathbf{z}_t(k)$ and the pre-compensated channel $\mathbf{z}_f(k)$ as in (17).

At the receiver (i.e. vehicle), we can recognize the following two situations:

1) *Ideal case:* If the predicted channel at the RSU is exactly same as the true $\mathbf{z}_t(k)$ with no noise or errors, then the estimated channel will have a perfect flat surface.
2) *Practical case*: In reality, due to the presence of additive noise, prediction and estimation errors, the estimated channel will not be perfectly flat but will be orders of magnitude better compared to receiver-side equalization only.

The estimated channel $\mathbf{z}_f(k)$ is piggybacked on acknowledgment frames back to the RSU where it computes the measurement channel $\mathbf{z}(k)$ as per (19), by combining (15) and (17). This forms the new input to the Kalman filter in (5).

$$\mathbf{z}(k) = \mathbf{z}_f(k) \odot \mathbf{z}_p(k) + \mathbf{w}(k) \tag{18}$$

$$= \mathbf{z}_f(k) \odot \frac{1}{\tilde{\mathbf{z}}_p(k)} + \mathbf{w}(k) \tag{19}$$

where, $\mathbf{w}(k)$ is an additive term that captures the difference between the true and the measured channels. Figure 5 shows the measurement channel generation process.

V. Results

The vehicular Edge network in Figure 1, is modeled using an open source GSCM simulator, *Quadriga* [19]. All the results are for the center location of the road since it represents the worst case scenario in terms of the scattering zone as defined in II-A. The AR-model order is $p = 3$, and the target vehicle's speed is $V = 20$ m/s (45 mph). Further, the road length is set to $d_{road} = 200$ m and the RSU is 1 m above the target vehicle's antenna height, which is 1.5 m from the surface of the road (i.e $d_{RSU} = 2.5$ m). The road length is divided into 20 segments (i.e. $d_{seg} = 10$ m). The number of variable scatterers is modeled as a random variable between 0 and 15; however, the number of fixed scatterers is assumed to be 5 (deterministic road-side features). The road is assumed to be identical on both sides of the RSU, which is placed at the center of the road. It is also assumed that there is a LOS propagation and the RSU-vehicle communication link is not intercepted by large vehicles.

Figure 6 shows the performance of the tracking and prediction algorithm. Figure 6a shows the error between the predicted channel coefficients and the true channel as generated by Quadriga, given by $\mathbf{e}(k) = \mathbf{z}_t(k) - \mathbf{z}_p(k)$. The variance in error is plotted for all the subcarriers for 100 channel instances. The variance about the median error value is uniform across subcarriers. Further the median value of the prediction error remains fairly constant. This shows that the prediction algorithm is indeed able to track the non-stationary V2I channel with high accuracy.

Figure 6b compares the error performance with and without (as in 802.11p) predictive analytics. In both the cases the widely used pilot-based linear interpolation equalization is employed at the receiver. The BER corresponds to an OFDM packet of 100 bits modulated using BPSK-1/2 modulation and coding at a carrier frequency of $f_c = 5.9$GHz and sampling frequency of $f_s = 10$MHz. As shown in Figure 6b, combining prediction and pre-compensation the frequency selective fading of the V2I channel is very well compensated that results in a BER improvement by two orders of magnitude. In contrast the conventional receiver algorithms are simply not sufficient to track the channel over of time and frequency. Hence those performs much worse even at high SNR. This is another motivating reason to adopt RSU-based prediction and pre-compensation. The ideal scenario represents an oracle with complete knowledge of the channel properties, which is shown for comparison. The predictive analytics employed in this work requires only 10 dB more SNR to achieve the same BER (10^{-3}) as the ideal case, which is very encouraging. Figure 6c, shows the estimated channel at the receiver. The almost ideal flat fading at the receiver leads to superior BER performance shown in Figure 6b. The linearity is piece-wise because the channel is estimated at the pilot carriers and interpolated for other subcarriers. However, the overall flatness of the estimated channel is sufficient to greatly improve the BER. Therefore, from these results, it is evident that by using predictive analytics at the RSU, V2I communication can be greatly improved and this increased reliability enables many new network services that currently suffer from time-varying, non-stationary channel characteristics.

VI. Related Work

Impairments in V2X channels, like shadowing by other vehicles, high Doppler, and inherent non-stationarity, impact

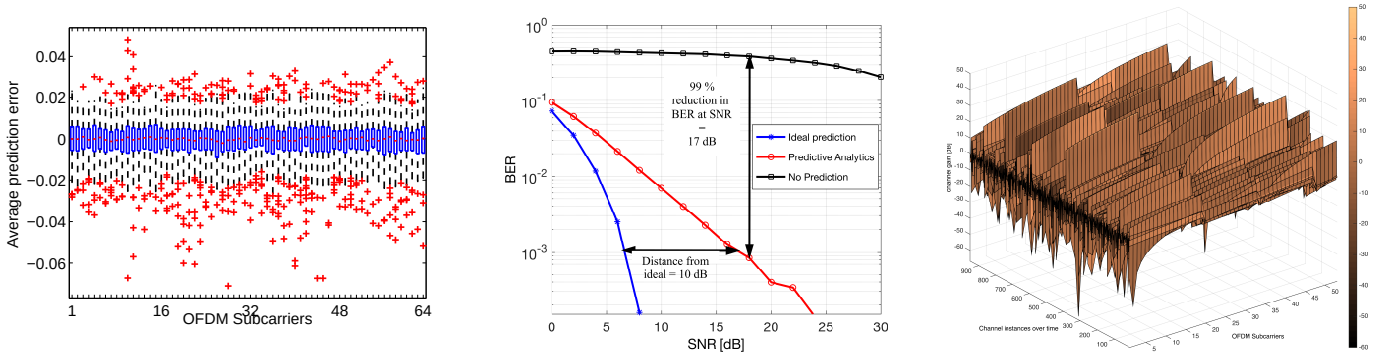

(a) Prediction error (b) BER comparison (c) Equalized channel at the vehicle

Figure 6: Performance of predictive analytics at RSU: 1) The statistics of prediction error are stationary across the OFDM subcarriers, which shows accurate tracking by the prediction algorithm. 2) The BER with predictive analytics is almost *two orders of magnitude* lower than conventional methods used in 802.11p. Also, it requires only 10 dB more SNR to achieve the same low BER of 10^{-3} as the ideal case (perfect estimation). 3) The estimated channel is largely flat channel that improves channel estimation using standard pilot carriers, ultimately improving the BER.

the reliability and latency of data transmission [20], which has also been validated by various measurement campaigns [8] In [21], an L-path Rayleigh channel model is used to model an OFDM system operating on fast time-varying vehicular environment, and the extended Kalman filter is used for recursive channel estimation. However, this model presumes a deterministic evolution of the coefficients [15]. In this paper, we use WINNER channel model [14], which is a more realistic and generic channel model than the theoretical models, such as Rayleigh model, to represent the vehicular channel between a RSU and a moving vehicle.

Conventional pilot based channel estimation and equalization techniques employed by DSRC are not sufficient to combat the V2I channel inefficiencies. These methods of estimation work best for channels where the fading profile between the pilot subcarriers is mostly flat or at least linear, which allows for linear interpolation techniques to estimate the channel using pilots. Non-linear methods [22] often add receiver complexity and unsuitable for hardware implementation. Furthermore, Decision Feedback Equalization (DFE) [23], [24] provides better results at the cost of complex feedback paths in the receiver and are more suited to networks that can sustain a higher processing latency, like LTE. Hence, we need novel algorithms for V2I channel shown in figure 3c.

VII. Practical System Implication

In this work, the evaluation of the V2I channel prediction system is focused on one location within the FSR. However, this techniques can be easily extended to build complete system of multiple vehicles and segments. We provide a brief sketch of the various steps that are required in integrating the predictive analytics into a real-time vehicular network. Most of these are currently being investigated using simulation and practical channel measurements.

Tracking and prediction over multiple segments: As the target vehicle moves along the road, it crosses the boundary between neighboring segments. Since the channel is quasi-stationary within the length of a segment but non-stationary over adjacent segments the proposed predictive technique can be used in two ways: 1) Use separate tracking and prediction kernels for each road segment following the algorithm described in §III and §IV. Since the prediction algorithm continuously assimilates CSIs over time, the RSU will always have the last predicted channel for a particular segment. Once a vehicle enters a segment, a new CSI feedback will trigger a re-computation of the prediction for the next downlink transmission. Therefore, there is no wait time at the RSU for training. 2) Alternatively, one analytics engine can be used for the entire stretch of the road. In that case, a database of the previously recorded CSIs is required to assist the prediction algorithm to arrive at a steady state. The last CSI received from the previous segment is used as the initial state. Once steady-state is achieved the remainder of the algorithm follows the steps discussed in previous sections and starts to update the prediction based on the database recorded for the current segment (as in Table I). However, This option is only feasible if the target vehicle is moving slowly and the RSU has large computational resources.

Tracking and prediction for multiple vehicles: In the multiple vehicle scenario, multiple prediction engines are required, where the number of tracking engines will depend on the number of vehicles N_v that needs to be tracked simultaneously. However, due to quasi-stationarity of channel within one segment, if all of the N_v vehicles are in one segment, then only one tracking engine is sufficient. However, if the vehicles are in different segments (more practical setting), then each segment needs to track its set of vehicles separately from the other segments. Since the GSCM channel model suggests that the segment length to be approximately 10 meters, the number of tracking engines to be supported at the RSU is dependent on the coverage area of the RSU (e.g. transmit power, carrier frequency, etc). We believe that with advances in virtualization of edge networks the system can be made highly scalable.

Simultaneous multiuser downlink: Although the V2I channel can be tracked and predicted accurately, it is mandatory to have multiuser downlink communication to take full advantage of this system. Multiuser-MIMO (MU-MIMO) can take advantage of the predicted channel states provided by our design to precode waveforms to increase spatial multiplexing in a dense vehicular network. This will eliminate training for channel states that is required for MU-MIMO downlink. The online learning framework in our techniques is especially suitable for multiuser downlink.

Extension to V2V channel: The V2I learning framework can be extended to V2V as well. the channel dynamics is dictated by similar factors as in V2I except for transmit power, which will define the scattering zone. Also, since the prediction requires the knowledge of vehicle topology, the RSU or a cloud based infrastructure should share this information with each vehicle. To alleviate congestion, out of band communication (like cellular backhaul) should be used.

VIII. Conclusion and Future work

In this work, we have shown the power of predictive analytics when applied to highly dynamic wireless environments like V2I networks. By embedding the CSI in the acknowledgment frame, the RSU obtains an estimate of the fading environment for a specific segment of the road, which is assimilated over time to learn the channel coefficients. This allows the RSU to carefully tune the channel coefficients to compensate for the frequency selective fading and improve the BER of the downlink channel. The ability to combat the non-stationary V2I channel further opens new dimensions of research in intelligent Edge networks with implications in broad areas of communication and network systems.

Although the predictive algorithm perform very well in simulation, we are building a real-time, mobile vehicular network testbed in and around the university campus to study practical V2I channels. Vehicles are equipped with signal acquisition instruments that emulates the on-board units while road-side units are mounted on poles and other road-side locations at regular intervals. The scatterers are derived using a combination of open source GIS databases like OpenStreetMap [25] for road-side features and digital cameras to capture mobile scatterers (neighboring vehicles). Experiments are being conducted in different scattering densities, from residential areas to busy downtown locations at different times of the day. We believe that analysis of these practical measurements will further improve the accuracy of the predictive framework presented in this paper. The testbed will also enable research in proactive content caching, multiuser scheduling and other edge networking paradigm.

References

[1] Google Inc., "Google Self-Driving Car Project." [Online]. Available: http://www.google.com/selfdrivingcar/

[2] R. Robinson and F. Dion, "Michigan Department of Transportation Multipath SPAT Broadcast Project," Tech. Rep. 108002, 2013.

[3] L. M. Vaquero and L. Rodero-merino, "Finding your Way in the Fog : Towards a Comprehensive Definition of Fog Computing," vol. 44, no. 5, pp. 27–32, 2014.

[4] T. H. Luan, L. Gao, Z. Li, Y. Xiang, and L. Sun, "Fog Computing: Focusing on Mobile Users at the Edge," 2015. [Online]. Available: http://arxiv.org/abs/1502.01815

[5] R. Yu, Y. Zhang, S. Gjessing, W. Xia, and K. Yang, "Toward Cloud-based vehicular networks with efficient resource management," *IEEE Network*, vol. 27, no. 5, pp. 48–55, 2013.

[6] A. Ashok, P. Steenkiste, and F. Bai, "Enabling Vehicular Applications using Cloud Services through Adaptive Computation Offloading," 2015.

[7] Intelligent Transportation System America, "Intelligent Transportation System America - http://www.itsa.org/." [Online]. Available: http://www.itsa.org/

[8] M. Boban, T. T. V. Vinhoza, M. Ferreira, J. Barros, and O. K. Tonguz, "Impact of vehicles as obstacles in Vehicular Ad Hoc Networks," *IEEE Journal on Selected Areas in Communications*, vol. 29, no. 1, pp. 15–28, 2011.

[9] M. Boban, J. Barros, and O. K. Tonguz, "Geometry-Based Vehicle-to-Vehicle Channel Modeling for Large-Scale Simulation," vol. 63, no. 9, pp. 4146–4164, 2014.

[10] IEEE Computer Society : LAN/MAN Standards Committee, *Part 11: Wireless LAN Medium Access Control (MAC) and Physical Layer (PHY) Specifications, Amendment 6: Wireless Access in Vehicular Environments (WAVE)*, 2010.

[11] X. Wu, S. Subramanian, R. Guha, R. G. White, and S. Member, "Vehicular Communications Using DSRC : Challenges , Enhancements , and Evolution," vol. 31, no. 9, pp. 399–408, 2013.

[12] LAN/MAN Standards Committee, S. Committee, and I. Computer, *Part 11 : Wireless LAN Medium Access Control (MAC) and Physical Layer (PHY) S pecifications*, 2012, vol. 2012, no. March.

[13] L. C. L. Cheng, B. Henty, R. Cooper, D. Stancil, and F. B. F. Bai, "Multi-Path Propagation Measurements for Vehicular Networks at 5.9 GHz," *2008 IEEE Wireless Communications and Networking Conference*, pp. 1239–1244, 2008.

[14] T. Svensson, M. Werner, R. Legouable, T. Frank, and E. Costa, "Ist-4-027756 Winner Ii," *Projects.Celtic-Initiative.Org*, vol. 1, no. 206, pp. 1–206, 2007. [Online]. Available: http://projects.celtic-initiative.org/WINNER+/WINNER2-Deliverables/D4.6.1.pdf

[15] M. Arnold, W. H. R. Miltner, H. Witte, R. Bauer, and C. Braun, "Adaptive AR modeling of nonstationary time series by means of Kalman filtering," *IEEE Trans. Biomed. Eng.*, vol. 45, no. 5, pp. 545–552, 1998.

[16] M. Sternad and D. Aronsson, "Channel Estimation and Prediction for Adaptive OFDM Downlinks," *Veh. Technol. Conf. 2003. VTC 2003-Fall. 2003 IEEE 58th*, vol. 2, pp. 1283–1287, 2003.

[17] M. McGuire and M. Sima, "LOW-ORDER KALMAN FILTERS FOR CHANNEL ESTIMATION," in *Commun. Comput. signal Process. 2005. PACRIM. 2005 IEEE Pacific Rim Conf.*, no. 1, 2005, pp. 8–11.

[18] M. Verhaegen and P. Van Dooren, "Numerical Aspects of Different Kalman Filter Implementations," *IEEE Trans. Automat. Contr.*, vol. AC-31, no. October, pp. 1–11, 1986.

[19] D. Revision, "Quasi Deterministic Radio Channel Generator User Manual and Documentation," pp. 1–116, 2015. [Online]. Available: http://www.quadriga-channel-model.de

[20] C. F. Mecklenbraüker, A. F. Molisch, J. Karedal, F. Tufvesson, A. Paier, L. Bernadó, T. Zemen, O. Klemp, and N. Czink, "Vehicular channel characterization and its implications for wireless system design and performance," *Proceedings of the IEEE*, vol. 99, no. 7, pp. 1189–1212, 2011.

[21] E. Simon, H. Hijazi, L. Ros, M. Berbineau, E. Simon, H. Hijazi, L. Ros, M. Berbineau, J. Estimation, E. P. Simon, H. Hijazi, L. Ros, and M. Berbineau, "Joint Estimation of Carrier Frequency Offset and Time-varying Vehicular Environments Joint Estimation of Carrier Frequency Offset and Channel Complex Gains for OFDM Systems in Fast Time-varying Vehicular Environments," 2010.

[22] S. Coleri, M. Ergen, A. Puri, and A. Bahai, "Channel estimation techniques based on pilot arrangement in OFDM systems," in *Broadcasting, IEEE Transactions on*, vol. 48, pp. 223–229.

[23] K. Sil, M. Agarwal, D. Guo, M. L. Honig, and W. Santipach, "Performance of turbo decision-feedback detection for downlink OFDM," *IEEE Wireless Communications and Networking Conference, WCNC*, pp. 1488–1492, 2007.

[24] R. Budde and R. Kays, "Delayed Decision Feedback Equalization with Adaptive Noise Filtering for IEEE 802 . 11p," pp. 17–23, 2013.

[25] O. S. Map, "Open Street Map - https://www.openstreetmap.org/." [Online]. Available: https://www.openstreetmap.org/